Acta Cryst. (1990). B46, 209–215

Phase Improvement in the Structure Interpretation of Fragment TR_2C from Bull Testis Calmodulin using Combined Entropy Maximization and Solvent Flattening

BY LENNART SJÖLIN AND L. ANDERS SVENSSON

Department of Inorganic Chemistry, Chalmers University of Technology and University of Göteborg, S-412 96 Göteborg, Sweden

EDWARD PRINCE

Reactor Radiation Division, National Institute of Standards and Technology, Gaithersburg, MD 20899, USA

AND STAFFAN SUNDELL

Department of Structural Chemistry, Faculty of Medicine, University of Göteborg, PO Box 33 031, S-400 33, Göteborg, Sweden

(*Received* 3 *February* 1989; *accepted* 26 *June* 1989)

Abstract

Fragment TR_2C (residues 78–148) of bull testis calmodulin ($M_r = 8260$ daltons) crystallizes in space group $P4_32_12$ with $a = 52{\cdot}4$ (1) and $c = 130{\cdot}0$ (1) Å, with two complete molecules in the asymmetric unit. After unsuccessful attempts to find a satisfactory starting set of phases using single-isomorphous-replacement and single-anomalous-scattering methods, a set of phases was found from one solution obtained by standard molecular-replacement methods, using the structure of troponin C as the starting model. The second independent molecule was found from Fourier maps based on maximum-entropy calculations and the startset of phases from the molecular-replacement calculations. The present structure has been refined at 3·6 Å resolution with 1420 independent reflections to $R = 0{\cdot}257$. The molecular conformation is very similar to that of the corresponding part of the intact parent protein calmodulin.

Introduction

The calcium-binding protein calmodulin is widely distributed in eukaryotic systems, where it combines with, and modulates the activity of, many different enzymes (Cheung, 1980; Walsh & Hartshorne, 1983; Manalan & Klee, 1984). We have been particularly interested in a process involving myosin light-chain kinase that plays a central role in the activation of myosin.

Although the determination of the three-dimensional structure of calmodulin has been reported (Babu, Sack, Greenhough, Bugg, Means & Cook, 1985), the complete set of coordinates has only recently become available in the public domain. We have chosen to study fragment TR_2C (residues 78–148) from bull testis calmodulin for several reasons. First, if a smaller fragment contains plausible drug-binding sites, it is clearly simpler to work with it, but it is very important to determine if the fragment has the same structure as the corresponding part of the complete molecule. Also, if ^{113}Cd nuclear magnetic resonance (NMR) is to be a valid approach to the analysis of the calcium-binding properties of the intact protein (Andersson, Forsén, Thulin & Vogel, 1983), it is important that the fragment closely resembles the corresponding part of the parent molecule. Finally, because of the difference in size, the dynamical properties of the fragment can be more easily studied by two-dimensional NMR (Wagner & Wüthrich, 1982; Wagner, 1983) than can those of the complete molecule.

Starting from a set of phases determined by the use of molecular replacement, a new algorithm (Prince, Sjölin & Alenljung, 1988) was used, in combination with solvent flattening, to maximize the entropy (Collins, 1982; Wilkins, Varghese & Lehmann, 1983; Bricogne, 1984) of low-resolution F_o and $2F_o - F_c$ maps in order to extend phases to higher resolution. The resulting density maps were successfully interpreted.

This paper describes the determination of the structure of fragment TR_2C of bull testis calmodulin at 3·6 Å resolution. Because it is one of the first examples of the application of this method of entropy maximization to the determination of phases for a previously unknown structure, the procedure used is described in detail.

0108-7681/90/020209-07$03.00

Experimental

Purification

Fragment TR_2C (residues 78–148) from bull testis calmodulin was prepared according to a method described by Andersson *et al.* (1983). Proteolytic fragmentation of calmodulin with trypsin followed the procedures described by Drabikowski, Brzeska & Venyaminov (1982) and by Walsh, Stevens, Kuznicki & Drabikowski (1977). Typically, 1 mg of trypsin was added to 100 mg of calmodulin dissolved in 100 ml of a freshly prepared solution of 100 m*M* NH_4HCO_3 and 1 m*M* $CaCl_2$, pH 7·8. The reaction was stopped after 35 min at room temperature by the addition of 2 mg of soybean trypsin inhibitor. Fragments were purified on a DEAE-Sephadex A-25 column* (equilibrated in 50 m*M* KH_2PO_4, pH 7·2) that was eluted with a linear NaCl gradient up to a concentration of 0·5 *M*. Under these conditions calmodulin completely disappeared, and the peptide TR_2C was the last fraction eluted from the column. Peptides were checked for purity by sodium dodecyl sulfate gel electrophoresis and agarose gel electrophoresis in the presence of Ca^{2+}.

Crystallization

For the crystallization experiments highly purified water (Milli-Q®) was used, and the lyophilized protein was dissolved to a concentration of 15 mg of protein per ml of water. A reservoir solution containing 24% of poly(ethylene glycol) 4000 (PEG 4000), 0·1 *M* acetate buffer solution (pH = 4·7) and 0·1 *M* of $CaCl_2$ was then prepared. The crystals grew from drops hanging from the covers of Petri dishes (Rayment, 1985); the droplets were initially formed by mixing 6 μl of protein solution with 4 μl of reservoir solution. Usually one large crystal grew in each droplet when the Petri dishes were held at room temperature. Crystallization experiments were also performed at 278 K, but no enhanced crystal quality or growth could be obtained.

The growth experiments produced crystals that crystallized in the tetragonal space group $P4_12_12$ or in its enantiomorph, $P4_32_12$, with cell dimensions $a = b = 52{\cdot}4$ (1) and $c = 130{\cdot}0$ (1) Å. The crystals grew to their maximum size (about 1·5 × 1·0 × 0·5 mm) within 14 d.

If we assume that there are two molecules with molecular weight 8260 daltons in the asymmetric unit, and that the protein density is about 1·35 g ml^{-1}, the volume of the protein in the asymmetric unit is about 20300 $Å^3$. The volume of the asymmetric unit is about 44600 $Å^3$, thus the solvent fraction is 55·4%, which is well within the range given by Matthews (1968). Other assumptions about the number of molecules in the asymmetric unit lead to values far outside the established range. Crystallographic data are given in Table 1.

Table 1. *Crystallographic data for fragment TR_2C from bull testis calmodulin*

Crystallization conditions	24% poly(ethylene glycol) 4000 0·10 *M* acetate buffer, pH = 4·7 0·10 *M* $CaCl_2$
Protein concentration	15 mg ml^{-1}
Space group	$P4_32_12$
Cell constants	$a = b = 52{\cdot}4$, $c = 130$ Å
M_r	8260 daltons
Water content	55%
Molecules per asymmetric unit	2
Resolution of data	3·6 Å

A heavy-atom-derivative crystal was prepared by slowly adding a K_2PtCl_6 solution to the crystallization vial.

Data collection

The crystals were mounted in thin-walled glass capillaries, the excess of solvent was dried out, and, in addition, synthetic mother liquor was added on one side of the capillary. Precession photographs were taken with a Nonius camera with a crystal-to-film distance of 100 mm. On these films the crystals were observed to be tetragonal. 00*l* reflections were observed only for $l = 4n$ and *h*00 reflections were observed only for $h = 2n$. It was concluded that the space group was $P4_12_12$ or $P4_32_12$.

Diffraction data for the native crystal were collected at room temperature with an Enraf–Nonius CAD-4 single-crystal diffractometer. The intensities of 1420 independent reflections were measured to a nominal resolution of 3·6 Å using graphite-monochromatized Cu $K\alpha$ radiation ($\lambda = 1{\cdot}5418$ Å). Because of the relatively large unit-cell dimensions, the reciprocal space is fairly densely populated, so an elongated 2θ arm was used to enable resolution of the intensity peaks. The scattered X-ray beam was passed through a tube filled with helium gas.

Integrated intensities were calculated using a modified version of program *LEOMA* (Andersen, 1985) in which the method of Lehmann & Larsen (1974) was used for strong reflections, while the dynamic mask procedure of Sjölin & Wlodawer (1981) was applied to medium and weak reflections. The program was modified to operate interactively, and reflections with skewed peaks were automatically displayed (or plotted) on a terminal screen for subsequent correction. Since the crystals seemed to be rather radiation sensitive, data were collected in three steps according to a procedure described by

* Certain commercial equipment, instruments and materials are identified in this paper in order to specify the experimental procedure. Such identification does not imply recommendation or endorsement by the National Institute of Standards and Technology, nor does it imply that the equipment or material identified are necessarily the best for the purpose.

Hendrickson (1976). First, as a reference, the *hk*0 plane of data was collected, followed by collection of the main body of the data, during which three standard reflections were measured after every 100th reflection. The total time, t, of exposure to the X-ray beam was recorded each time the standard reflections were measured. The standard reflections decayed roughly 20% during the data collection. Finally, the *hk*0 plane was recollected, and radiation damage was corrected for according to

$$R(t,s) = \exp(-kt)\,[1 + kt\,\exp(-Ds^2)], \qquad (1)$$

where D is the root-mean-square displacement of the atoms, $s = (\sin\theta)/\lambda$ and k is the rate constant whose value is determined from the *hk*0 data. The standard reflections were then reanalyzed and it was found that the radiation-damage calculations based on the *hk*0 planes had brought all three standard reflections to an almost completely correct level. The integrated intensities of all reflections were then corrected for absorption using the pseudo-empirical method described by North, Phillips & Mathews (1968).

The derivative crystal was mounted in a capillary, and data to 3·6 Å resolution were collected using the same procedure as for the native crystal. The unit-cell parameters for the derivative crystal were measured to be $a = 52{\cdot}2$ (1), $c = 129{\cdot}8$ (2) Å. In addition, Friedel mates to be used for anomalous-dispersion analysis were collected following procedures described by Hendrickson (1985). In order to minimize systematic errors between anomalous pairs, h, k, l and $-h$, $-k$, $-l$ reflections were measured close in time and at settings of nearly equivalent absorption. Anomalous pairs were measured for the centric reflections as well, to establish the noise level for the anomalous signal. The *hkl* structure amplitudes were scaled to their *hkl* mates using a modified algorithm of the local scaling type according to Matthews & Czerwinsky (1975). The anisotropic scale factors were calculated separately for $(\sin\theta)/\lambda$ shells of data. A comparison of the r.m.s. anomalous differences for centric and acentric data revealed immediately the magnitude of the observed anomalous-scattering signal, which could in turn be compared with the expected value. Table 2 shows the resulting calculation of the magnitudes of the anomalous signal. As can be seen from Table 2, there is a measurable anomalous signal in the heavy-atom-derivative data set. According to previous analyses (Hendrickson & Teeter, 1981; Hendrickson, Smith & Sheriff, 1985), this signal should have been sufficient for phasing purposes.

Table 2. *Result from local scaling of the anomalous data and the subsequent analysis of the anomalous signal*

The signal for the acentric data is presented. DELBAR = $\Sigma(|F_{PH\cdot}| - |F_{PH}|)/n$. RMSDEL = $[\Sigma(|F_{PH\cdot}| - |F_{PH}|)^2/n]^{1/2}$. RMSSIG = $\{\Sigma[(\sigma_{PH\cdot})^2 + (\sigma_{PH})^2]/n\}^{1/2}$. SIGNAL = $(\text{RMSDEL}^2 - \text{RMSSIG}^2)^{1/2}$.

Resolution d_{min}	No. of observations	Average	RMSF	DELBAR	RMSDEL	RMSSIG	SIGNAL
9·13	9	639	710	31	41	34	24
7·07	50	695	772	38	47	39	27
5·81	58	460	487	40	50	49	8
5·09	68	530	568	48	63	58	23
4·66	68	545	577	48	62	58	21
4·32	67	571	599	53	78	63	46
4·04	80	604	626	58	82	70	43
3·60	60	585	609	67	93	75	55
Total	460	569	608	51	70	61	36

Maximum entropy

Various workers (Collins, 1982; Wilkins, Varghese & Lehmann, 1983; Bricogne, 1984) have suggested that the maximum-entropy method provides an approach to the determination of the distribution of the electron density in a crystal when only the amplitudes of its Fourier transform can be measured, and those only in a bounded region of reciprocal space. Consider a unit cell with volume V divided into N 'pixels', and let ρ_k be the mean density in the kth pixel. The maximum-entropy method consists of finding the maximum of

$$S = -\sum_{k=1}^{N} \rho_k \ln \rho_k \qquad (2)$$

subject to the condition that the sum over the unit cell of $(V/N)\rho_k$ is equal to $F(000)$ and to one or more other conditions that require approximate agreement with the observed data. Wilkins, Varghese & Lehmann (1983), following Gull & Daniell (1978), proposed that the second condition be a 'weak' constraint of the form

$$\sum_{j=1}^{M} [|F_{oj}| - |F_{cj}|]^2/\sigma_j^2 \le M, \qquad (3)$$

where F_{oj}, F_{cj} and σ_j are, respectively, the observed and calculated structure factors and the standard deviation of the observed structure factor of reflection j, and the sum is over a set of M reflections.

An attempt was made to improve the density map for fragment TR_2C using the method of the 'single-pixel equation' described by Wilkins (1983). The procedure proved to be computationally cumbersome, but the results were sufficiently promising to make it seem worthwhile to try to develop a more efficient solution to the maximum-entropy problem. The method used has been described in detail by Prince, Sjölin & Alenljung (1988), so only a brief summary will be given here. Consider the function

$$E(\rho) = \sum_{k=1}^{N} \rho_k \sum_{j=1}^{M} |F_{oj}| \cos(2\pi \mathbf{h}_j.\mathbf{r}_k - \varphi_j), \qquad (4)$$

which is the expected value for the distribution $\rho(\mathbf{r})$ of a truncated Fourier series in which $|F_{oj}|$ is the

observed amplitude for a reflection whose indices are $\mathbf{h}_j$, and whose previously estimated phase is φ_j. Prince, Sjölin & Alenljung (1988) showed that if φ_j is the correct phase for F_{oj},

$$E(\rho) = \sum_{j=1}^{M} |F_{oj}|^2 \qquad (5)$$

and that entropy is maximized for constant $E(\rho)$ if

$$\rho_k = NF(000)\exp(z_k x)/V \sum_{l=1}^{N} \exp(z_l x), \qquad (6)$$

where

$$z_k = (\rho'_k - \rho'_1)/(\rho'_2 - \rho'_1) \qquad (7a)$$

$$\rho'_k = \sum_{j=1}^{M} |F_{oj}| \cos(2\pi \mathbf{h}_j.\mathbf{r}_k - \varphi_j) \qquad (7b)$$

and

$$x = \ln(\rho_2) - \ln(\rho_1) = \ln(\rho_2/\rho_1). \qquad (7c)$$

ρ_1 and ρ_2 are the densities in any pair of pixels for which the values of ρ'_k are different, although optimum numerical conditioning is achieved if they are chosen as the minimum and maximum values of ρ'_k, respectively. $E(\rho)$ is a smooth monotonically increasing function of x; Prince *et al.* (1988) give an expression for $dE(\rho)/dx$ with which (5) can be easily solved using Newton–Raphson or similar numerical methods.

Structure determination

In the first attempt to determine phases, heavy-atom positions were determined from difference Patterson maps and difference Fourier maps in the usual manner (Blundell & Johnson, 1976). Heavy-atom positional parameters were also obtained using the direct-methods program *MITHRIL* (Gilmore, 1984). Because the results from the interpretation of the Patterson maps and from direct methods were similar, positional parameters, isotropic temperature factors and occupancies were then refined using the methods of Dickerson, Weinzierl & Palmer (1968). The result from this refinement is summarized in Table 3. Because there was only one derivative data set, a phase set was recalculated from the refined parameters (Wang, 1985), giving a statistical figure of merit of 0·48. From this phase set a Fourier map was calculated, and a tentative molecular envelope was calculated that, in order to avoid including protein in the solvent region, assumed that 35% of the volume of the unit cell was solvent. Several cycles of solvent flattening and envelope recalculation gave results that are summarized in Table 4. A 3·6 Å density map was then calculated using centroid phases (Blow & Crick, 1959) and structure amplitudes weighted by the individually calculated figures of merit. The overall figure of merit for 826 observed single-isomorphous-replacement (SIR) pairs was 0·79, but the quality of the resulting maps was poor, and chain-tracing attempts were not successful.

Table 3. *Phase-refinement results for* 826 *unique reflections within a resolution of* 15·0 *to* 4·0 Å

Derivative	Site no.	Occupancy	Temperature factor (Å²)	x	y	z
K_2PtCl_6	1	48·5	15·0	0·1240	0·3430	0·6965
	2	27·4	15·0	0·3115	−0·0094	0·8968
	3	22·9	15·0	0·3420	0·0881	0·0390
	4	18·5	15·0	0·9403	0·3338	0·4003
	5	12·7	15·0	0·3282	0·1714	0·4444
	6	17·7	15·0	0·9507	0·2936	0·1015
	7	7·8	15·0	0·9871	0·2926	0·6835
	8	6·5	15·0	0·0480	0·0926	0·2615

Table 4. *Statistics obtained from solvent-flattening density modifications performed on fragment* TR_2C *to* 3·6 Å *resolution*

Cycle no.	Figure of merit	Phase shift (°)	Accumulated phase shift (°)
1	0·53	20·8	20·8
2	0·65	7·1	26·0
3	0·73	5·3	29·7
4	0·77	4·2	33·2
5	0·79	3·1	35·6

Table 5. *Summary of density modification according to Wang* (1985) *combined with maximum-entropy calculations from initial phases obtained with the ISIR method*

Cycle no.	R value (%)	Figure of merit	Phase shift (°)	Accumulated phase shift (°)	Map type
1	24·4	0·79	6·2	6·2	Wang
2	16·2	0·85	8·1	12·5	Max. entropy
3	18·5	0·82	4·4	14·9	Wang
4	11·3	0·90	4·8	18·0	Max. entropy
5	14·6	0·85	2·1	18·9	Wang
6	8·5	0·91	2·3	20·2	Max. entropy

The next approach to the determination of the structure was to use the final phase set obtained from the solvent-flattening procedure as input to maximum-entropy (ME) calculations using the algorithm described by Prince, Sjölin & Alenljung (1988). The phases were modified in a series of calculations according to the scheme summarized in Table 5. The analysis converged to a figure of merit of 0·91 and an agreement index between the inversion of the map and the observed amplitudes of 8·5%. Another electron density map was computed at a resolution of 3·6 Å, using the phases from the ME calculations and the observed amplitudes, but the attempt to fit a chain to the map was again unsuccessful.

Next, the anomalous-scattering data were used in a search for a satisfactory starting phase set. Pat-

terson maps were calculated based on the squared differences between Friedel pairs from noncentrosymmetric zones. The choice of plausible heavy-atom sites from this Patterson map did not match the solution obtained from the SIR data. The tentative solution from the anomalous Patterson maps was further tested in a least-squares refinement procedure, using a version of the program *ANOLSQ* (Hendrickson, 1985) that had been modified for our space group. However, these positions did not refine properly, and the anomalous-scattering data were therefore also discarded.

The final set of phases for fragment TR_2C of calmodulin was obtained by a combination of the molecular-replacement technique (Lattman, 1985) and ME calculations. Because C_α coordinates for calmodulin were not available at the time, and because there was reason to believe that troponin C would have a similar conformation, the latter structure was used as the starting model (Herzberg & James, 1985), and independent solutions were determined for rotational and translational parameters. The rotation parameters were determined using the rotation function of Rossman & Blow (1962). The function was sampled at 5° intervals, with 1° intervals used in the regions of correlation maxima to define the rotation angles more precisely. Because the asymmetric unit contains two molecules, a self-rotation calculation was also performed. The results of the molecular-replacement calculations are summarized in Table 6. After an analysis of the internal correlation between the rotation solutions, peak number 3 in Table 6 was selected, and the translational parameters for this solution were determined using an *R*-index-minimization search (Remington, unpublished program). These parameters were then subjected to rigid-body least-squares refinement using the program *ROTLSQ* (Hendrickson, personal communication). The refined position of the starting model, oriented in the TR_2C unit cell, gave an *R* index of 0·48. After the rigid-body refinement the atomic coordinates and an overall temperature factor were refined, keeping the molecular geometry rather tight, using the program *PROLSQ* (Konnert & Hendrickson, 1980). The resulting *R* index was 0·42. New phases were then calculated and entered into the density modification system, where they were subjected to solvent flattening and ME calculations. Table 7 presents the result of four cycles of calculation. In a new Fourier map calculated from this phase information it was immediately found that the envelope for the other molecule in the asymmetric unit was very well defined and placed in the allowed region of the unit cell. The new density showed nicely helical features and it was easily found that the solution from peak number 4 in Table 6, when translated in the unit cell, fitted rather satisfactorily into this electron density. The initial model from troponin C was now placed in the density from the two solutions and was consequently rebuilt and refined in a series of cycles. After adjusting the direction of the N- and C-terminus α-helices, the side chains were added to the main-chain structure in steps, when $2F_o - F_c$ Fourier maps showed clear density features. In order for helices to have the proper hand it was concluded that the correct space group was $P4_32_12$.

It was later found, after some additional calculations, that peak number 3 and peak number 4 in Table 6 are related in such a way that they satisfy a major peak in the self-rotation map.

Table 6. *Peaks from the molecular-replacement calculations of fragment TR_2C using a polypeptide model of troponin C*

The rotation angles κ, ψ and φ are according to Rossman & Blow (1962).

Peak no.	κ (°)	ψ (°)	φ (°)	Relative peak height
1	88	148	28	95
2	126	98	43	94
3	192	70	52	100
4	250	34	75	94

Table 7. *Summary of density modification according to Wang* (1985) *combined with maximum-entropy calculations from initial phases obtained with molecular-replacement calculations*

Cycle no.	*R* value (%)	Figure of merit	Phase shift (°)	Accumulated phase shift (°)	Map type
1	16·6	0·78	10·4	10·4	Wang
2	12·4	0·84	9·6	18·3	Max. entropy
3	14·9	0·81	6·3	22·5	Wang
4	9·8	0·88	2·1	23·0	Max. entropy

Results and discussion

Starting with the main chain and some side chains fitted to the final Fourier map, ten iterations of refinement and refitting gave a model with an *R* index of 0·257, and a root-mean-square deviation of bonded distances from ideal values of 0·035 Å. In view of the relatively low resolution we have not tried to fit any solvent molecules into the model.*

* Atomic coordinates and structure factors have been deposited with the Protein Data Bank, Brookhaven National Laboratory (Reference: 1TRC, R1TRCSF), and are available in machine-readable form from the Protein Data Bank at Brookhaven or one of the affiliated centres at Melbourne or Osaka. The data have also been deposited with the British Library Document Supply Centre as Supplementary Publication No. SUP 37033 (as microfiche). Free copies may be obtained through The Technical Editor, International Union of Crystallography, 5 Abbey Square, Chester CH1 2HU, England.

Fig. 1 shows the conformation of the α-carbon skeleton of fragment TR_2C of bull testis calmodulin and the corresponding part of the intact molecule, as reported by Babu *et al.* (1985). They appear to be very similar. Data have recently been collected to 2·0 Å resolution on a different crystal form, and further efforts to refine the structure will be directed to those data.

The current model is based on starting phases obtained from classical molecular-replacement calculations and maximum-entropy calculations using the algorithm of Prince, Sjölin & Alenljung (1988). Phases obtained from single-isomorphous-replacement or single-anomalous-scattering data were not sufficient to produce an interpretable map despite the fact that the overall figure of merit, after ME calculations, was 0·91. Solvent flattening is based on the idea that, if a contiguous solvent region is forced to be featureless, the phases will resemble the correct ones. Harrison, Wlodawer & Sjölin (1988) have shown, however, that phases derived from solvent flattening are critically dependent on the molecular transform, which is, in turn, dependent on the choice of the boundary between the solvent and the molecule. When using a solvent-flattening method, such as the one developed by Wang (1985), it is essential to start with an accurate mask. The molecular envelope also appears as a strong constraint in the ME calculations used here, so it may be the most important limitation during the application of density-modification methods in phase determination (Schevitz, Podjarny, Zwick, Hughes & Siegler, 1981; Bhat & Blow, 1983; Podjarny, Bhat & Zwick, 1987). The ME calculations gave satisfactory results in this study only when the starting set was accurate enough. Nevertheless, maximum entropy promises to become a powerful phase-determining tool when further experience with its use has been gained.

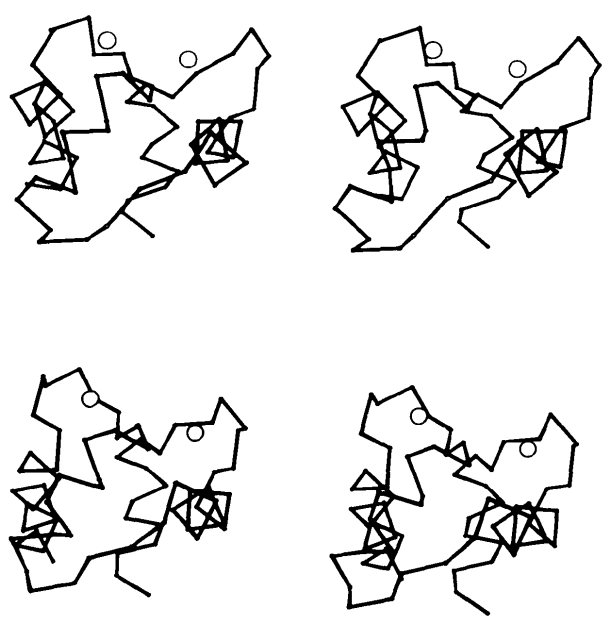

Fig. 1. Stereoscopic drawings of the backbone C_α atoms of the fragment TR_2C from bull testis calmodulin, represented in the upper field of the picture, and from the corresponding portion of the intact molecule of calmodulin represented in the lower field of the picture.

The authors thank Professor Sture Forsén and his colleagues for supplying TR_2C material and for many helpful suggestions. We also gratefully acknowledge Hässle AB for stimulating interest and supply of protein materials. We are indebted to Dr Vratislav Langer for valuable discussions concerning this work. Financial support has been provided by the Swedish Natural Science Research Council (Contract No. 4673).

References

ANDERSEN, L. (1985). Thesis, Univ. of Göteborg, Sweden.
ANDERSSON, A., FORSÉN, S., THULIN, E. & VOGEL, H. J. (1983). *Biochemistry*, **22**(10), 2309–2313.
BABU, Y. S., SACK, J. S., GREENHOUGH, T. J., BUGG, C. E., MEANS, A. R. & COOK, W. J. (1985). *Nature (London)*, **315**, 37–40.
BHAT, T. N. & BLOW, D. M. (1983). *Acta Cryst.* A**39**, 166–170.
BLOW, D. M. & CRICK, F. H. C. (1959). *Acta Cryst.* 794–802.
BLUNDELL, T. L. & JOHNSON, L. N. (1976). In *Protein Crystallography*, edited by B. HORECKER, N. O. KAPLAN, J. MARMUR & H. A. SCHERAGA. New York: Academic Press.
BRICOGNE, G. (1984). *Acta Cryst.* A**40**, 410–445.
CHEUNG, W. Y. (1980). *Science*, **207**, 19–27.
COLLINS, D. M. (1982). *Nature (London)*, **298**, 49–51.
DICKERSON, R. E., WEINZIERL, J. E. & PALMER, R. A. (1968). *Acta Cryst.* B**24**, 997–1003.
DRABIKOWSKI, W., BRZESKA, H. & VENYAMINOV, S. YU. (1982). *J. Mol. Chem.* **257**(19), 11584–11590.
GILMORE, C. J. (1984). *J. Appl. Cryst.* **17**, 42–46.
GULL, S. F. & DANIELL, G. J. (1978). *Nature (London)*, **272**, 686–690.
HARRISON, R. W., WLODAWER, A. & SJÖLIN, L. (1988). *Acta Cryst.* A**44**, 309–320.
HENDRICKSON, W. A. (1976). *J. Mol. Biol.* **106**, 889–893.
HENDRICKSON, W. A. (1985). In *Crystallographic Computing* 3, edited by G. M. SHELDRICK, C. KRÜGER & R. GODDARD, pp. 277–285. Oxford: Clarendon Press.
HENDRICKSON, W. A., SMITH, J. L. & SHERIFF, S. (1985). *Methods Enzymol.* **115**, 41–55.
HENDRICKSON, W. A. & TEETER, M. M. (1981). *Nature (London)*, **290**, 107–113.
HERZBERG, O. & JAMES, M. N. G. (1985). *Nature (London)*, **313**, 653–659.
KONNERT, J. & HENDRICKSON, W. A. (1980). *Acta Cryst.* A**36**, 344–350.
LATTMAN, E. (1985). *Methods Enzymol.* **115**, 55–77.
LEHMANN, M. S. & LARSEN, F. K. (1974). *Acta Cryst.* A**30**, 580–584.

MANALAN, A. S. & KLEE, C. B. (1984). *Adv. Cyclic Nucleotide Protein Phosphorylation Res.* **18**, 227–278.
MATTHEWS, B. W. (1968). *J. Mol. Biol.* **33**, 491–497.
MATTHEWS, B. W. & CZERWINSKI, E. W. (1975). *Acta Cryst.* A**31**, 480–487.
NORTH, A. C. T., PHILLIPS, D. C. & MATHEWS, F. (1968). *Acta Cryst.* A**24**, 351–359.
PODJARNY, A. D., BHAT, T. N. & ZWICK, M. (1987). *Annu. Rev. Biophys. Biophys. Chem.* **16**, 351–373.
PRINCE, E., SJÖLIN, L. & ALENLJUNG, R. (1988). *Acta Cryst.* A**44**, 216–222.
RAYMENT, I. (1985). *Methods Enzymol.* **114**, 136–140.
ROSSMAN, M. G. & BLOW, D. M. (1962). *Acta Cryst.* **15**, 24–31.
SCHEVITZ, R. W., PODJARNY, A. D., ZWICK, M., HUGHES, J. J. & SIEGLER, P. B. (1981). *Acta Cryst.* A**37**, 669–677.
SJÖLIN, L. & WLODAWER, A. (1981). *Acta Cryst.* A**37**, 594–604.
WAGNER, G. (1983). *Q. Rev. Biophys.* **16**, 1–57.
WAGNER, G. & WÜTHRISH, K. (1982). *J. Mol. Biol.* **160**, 343–361.
WALSH, M., STEVENS, F. C., KUZNICKI, J. & DRABIKOWSKI, W. (1977). *J. Biol. Chem.* **252**, 7440–7443.
WALSH, M. P. & HARTSHORNE, D. J. (1983). *Biochemistry of Smooth Muscle*, pp. 1–84. Boca Raton, FL: CRC Press.
WANG, B.-C. (1985). *Methods Enzymol.* **115**, 90–112.
WILKINS, S. W. (1983). *Acta Cryst.* A**39**, 892–896.
WILKINS, S. W., VARGHESE, J. N. & LEHMANN, M. S. (1983). *Acta Cryst.* A**39**, 47–60.

Acta Cryst. (1990). B**46**, 215–222

Structural Comparison of the Potent Antimuscarinic Agent Azaprophen Hydrochloride with Aprophen Hydrochloride and Structurally Related Antimuscarinic Agents

BY JEAN M. KARLE*

Department of Pharmacology, Division of Experimental Therapeutics, Walter Reed Army Institute of Research, Washington, DC 20307-5100, *USA*

ISABELLA L. KARLE

Laboratory for the Structure of Matter, Naval Research Laboratory, Washington, DC 20375-5000, *USA*

AND PETER K. CHIANG

Department of Applied Biochemistry, Division of Biochemistry, Walter Reed Army Institute of Research, Washington, DC 20307-5100, *USA*

(*Received* 4 *April* 1989; *accepted* 19 *September* 1989)

Abstract

A comparison of the crystalline structure of the potent azaprophen with the crystalline structures of aprophen and four other structurally related antimuscarinic agents reveals the potential for an ionic interaction of the cationic nitrogen atom and the carbonyl oxygen atom with the muscarinic receptor and an aromatic interaction with a phenyl group. 6-Methyl-6-azabicyclo[3.2.1]octan-3α-ol 2,2-diphenylpropionate hydrochloride (azaprophen hydrochloride), $C_{23}H_{28}NO_2^+.Cl^-$, $M_r = 385{\cdot}9$, monoclinic, $P2_1/c$, $a = 8{\cdot}490$ (1), $b = 14{\cdot}335$ (2), $c = 16{\cdot}847$ (2) Å, $\beta = 93{\cdot}63$ (1)°, $V = 2046{\cdot}2$ Å^3, $Z = 4$, $D_x = 1{\cdot}253$ g cm^{-3}, Cu $K\alpha$, $\lambda = 1{\cdot}54178$ Å, $\mu = 17{\cdot}86$ cm^{-1}, $F(000) = 824$, room temperature, final $R = 4{\cdot}25\%$ for 2460 reflections with $|F_o| > 3\sigma$. 2-Diethylaminoethyl 2,2-diphenylpropionate hydrochloride (aprophen hydrochloride), $C_{21}H_{28}NO_2^+.Cl^-$, $M_r = 361{\cdot}9$, orthorhombic, $Pbca$, $a = 15{\cdot}118$ (3), $b = 7{\cdot}488$ (2), $c = 36{\cdot}306$ (10) Å, $V = 4110{\cdot}8$ Å^3, $Z = 8$, $D_x = 1{\cdot}316$ g cm^{-3}, Cu $K\alpha$, $\lambda = 1{\cdot}54178$ Å, $\mu = 17{\cdot}45$ cm^{-1}, $F(000) = 1552$, room temperature, final $R = 7{\cdot}96\%$ for 1846 reflections with $|F_o| > 3\sigma$. Both azaprophen and aprophen were crystallized as tertiary amine salts. The overall conformation of both molecules is similar as demonstrated by space-filling models and superimposed stick drawings. Although the interatomic distance between the nitrogen atom and the carbonyl oxygen atom of azaprophen and aprophen is comparable at 5·41 and 5·07 Å, respectively, the nitrogen atoms of azaprophen and aprophen are 1·16 Å apart when the acyloxy portion (—O—C═O) of both molecules is superimposed. A conformational analysis of azaprophen, aprophen and the structurally similar antimuscarinic agents reveals a buried ether oxygen atom and an exposed carbonyl oxygen atom as well as the common placement of a phenyl group on the same side of the

* To whom correspondence should be addressed.

0108-7681/90/020215-08$03.00